

Knowledge Vector Weakening: Efficient Training-free Unlearning for Large Vision-Language Models

Yejin Kim¹ Dongjun Hwang¹ Sungmin Cha^{†2} Junsuk Choe^{†1}

Abstract

Large Vision-Language Models (LVLMs) are widely adopted for their strong multimodal capabilities, yet they raise serious concerns such as privacy leakage and harmful content generation. Machine unlearning has emerged as a promising solution for removing the influence of specific data from trained models. However, existing approaches largely rely on gradient-based optimization, incurring substantial computational costs for large-scale LVLMs. To address this limitation, we propose Knowledge Vector Weakening (KWW), a training-free unlearning method that directly intervenes in the full model without gradient computation. KWW identifies knowledge vectors that are activated during the model’s output generation on the forget set and progressively weakens their contributions, thereby preventing the model from exploiting undesirable knowledge. Experiments on the MLLM and CLEAR benchmarks demonstrate that KWW achieves a stable forget–retain trade-off while significantly improving computational efficiency over gradient-based and LoRA-based unlearning methods.

1. Introduction

Large Vision-Language Models (LVLMs) demonstrate strong performance across a wide range of multimodal tasks, including visual question answering (VQA), image captioning, multimodal retrieval, and document understanding (Liu et al., 2023; 2024a; Xue et al., 2024). Despite these advances, LVLMs raise critical concerns related to privacy leakage, copyright infringement, and the generation of harmful or inappropriate content (Brown et al., 2022; Eldan & Russinovich, 2023). To mitigate these risks, machine unlearning has emerged as a key paradigm that enables models to selectively remove the influence of problematic training

¹Sogang University ²New York University. Correspondence to: Junsuk Choe <jschoe@sogang.ac.kr>, Sungmin Cha <sungmin.cha@nyu.edu>.

data (Nguyen et al., 2022; Liu et al., 2024b).

Exact unlearning is the most straightforward approach to unlearning, which retrains a model from scratch after removing the forget data from the original training set. While this approach provides a clear conceptual solution, it is impractical in large-scale settings due to the prohibitive computational cost. To address this limitation, recent studies have focused on *approximate unlearning*, which aims to remove the influence of forget data from an already trained model without full retraining (Triantafillou et al., 2024). Most existing approaches adopt training-based strategies that compute gradients via backpropagation and update model parameters using optimization objectives (Thudi et al., 2022; Liu et al., 2025a; Zhang et al., 2024; Huo et al., 2025). However, for LVLMs, such methods remain computationally expensive in both time and memory, due to the need for fine-tuning large models (Wang et al., 2024a; Wilma et al., 2026).

To alleviate these challenges, recent unlearning approaches for large models increasingly rely on LoRA (Hu et al., 2022), a parameter-efficient fine-tuning (PeFT) techniques. While LoRA-based methods improve computational efficiency (Li et al., 2025; Cha et al., 2025; Kim et al., 2025b), they inherently restrict updates to a low-rank subspace. However, prior work (Shuttleworth et al., 2025) shows that parameter updates induced by LoRA are not uniformly distributed across the model, unlike full fine-tuning. Instead, these updates concentrate within a limited low-dimensional subspace, referred to as the intruder dimension. This suggests that the effects of LoRA-based optimization are only partially reflected in the model’s overall representational space compared to full fine-tuning.

These findings motivate a closer examination of LoRA-based approaches in the context of unlearning, where the objective is to efficiently remove specific knowledge from a model. When the knowledge to be removed is distributed not only within the intruder dimension but also across the broader representation space, an arbitrarily chosen LoRA rank can be insufficient to remove it effectively (§3). Consequently, such approaches expand the hyperparameter search space and incur higher computational costs, diminishing the efficiency benefits originally intended by LoRA.

To address these limitations, we propose Knowledge Vector Weakening (KVV), an efficient training-free unlearning method that directly intervenes in the full model using only forward propagation. Specifically, KVV identifies knowledge vectors in MLP modules that are accessed during forward passes on the forget set and attenuates their contribution to the output by scaling down these vectors. This process reduces the model’s reliance on the corresponding knowledge vectors and suppresses the associated knowledge access pathways. KVV does not require gradient computation or retraining, leading to substantial computational savings.

We evaluate our method on representative LVLM unlearning benchmarks, MLLMU-Bench (Liu et al., 2025a) and CLEAR (Dontsov et al., 2025). Experimental results show that KVV achieves more effective unlearning under retain performance constraints compared to gradient-based and LoRA-based methods. Moreover, KVV demonstrates clear advantages in terms of computational efficiency. In summary, our contributions are as follows:

- We introduce *Knowledge Vector Weakening (KVV)*, a gradient-free unlearning framework that achieves selective knowledge removal solely through forward propagation, eliminating the need for backpropagation or retraining.
- We propose a novel intervention strategy that identifies and progressively attenuates forget-related parameter vectors within MLP modules, thereby suppressing the neural pathways associated with the forget set.
- We demonstrate that KVV provides a superior forget–retain trade-off and significant computational savings compared to gradient-based and LoRA-based methods across representative LVLM benchmarks, including MLLMU-Bench and CLEAR.

2. Related Work

2.1. LLM Unlearning

LLM unlearning aims to remove the influence of specific data from large language models without costly retraining, addressing concerns such as privacy, copyright, and hazardous knowledge. Most existing methods rely on loss-function–based optimization, including Gradient Ascent (GA) (Thudi et al., 2022), Gradient Difference (GD) (Liu et al., 2025a), Negative Preference Optimization (NPO) (Zhang et al., 2024), and Inverted Hinge Loss (IHL) (Cha et al., 2025), which induce forgetting by manipulating gradients or token probabilities, though often at the cost of high computation and sensitivity to hyperparameters. Beyond loss-based approaches, alternative methods such as Task Arithmetic (Ilharco et al., 2023), decoding-time unlearning

with auxiliary models, and LoRA initialization techniques (Cha et al., 2025; Kim et al., 2025b) have been proposed.

These unlearning techniques for LLMs also form the foundation for subsequent research on unlearning in large vision–language models, as most LVLMs incorporate a pretrained LLM as their core language component.

2.2. LVLM Unlearning

Compared to LLM unlearning, research on LVLM unlearning remains at an early stage. Several benchmarks have recently been introduced to enable systematic evaluation, including MLLMU-Bench (Liu et al., 2025a), CLEAR (Dontsov et al., 2025), and FIUbench (Ma et al., 2025) for privacy-related unlearning, as well as PEBench (Xu et al., 2025) for event-scene unlearning.

From a methodological perspective, a small number of recent works explicitly incorporate visual information: MANU (Liu et al., 2025b) identifies important neurons via activation differences between multimodal and text-only inputs and prunes them, MMUnlearner (Huo et al., 2025) exploits gradient-based saliency induced by image-token ablation, and VKD (Wang et al., 2025) employs a teacher model to preserve intermediate visual representations on the retain set. However, these approaches typically require additional inference, retraining, or auxiliary models, resulting in substantial computational overhead. In contrast, our method achieves LVLM unlearning in a forward-only manner with significantly lower computational overhead.

3. Motivation

Most existing unlearning methods rely on training-based approaches that compute gradients via backpropagation and directly update model parameters using loss functions (Liu et al., 2025a; Zhang et al., 2024; Huo et al., 2025). In large-scale vision–language model settings, such approaches incur substantial computational overhead in both time and memory, which is further amplified by repeated training runs required for hyperparameter tuning.

To improve efficiency, several unlearning approaches adopt LoRA, a parameter-efficient fine-tuning (PeFT) technique. While these methods reduce the cost of parameter updates, they inevitably introduce additional hyperparameters, expanding the hyperparameter search space and undermining the original efficiency-oriented motivation of LoRA. In particular, the LoRA rank determines the subspace in which the model is modified. In unlearning settings, performance therefore becomes highly sensitive to how well this subspace aligns with the knowledge to be removed, as shown in Figure 1. We conduct experiments on the CLEAR benchmark (Dontsov et al., 2025) under a VQA setting using a 2-fold validation, motivated by (Cha & Cho, 2025). When

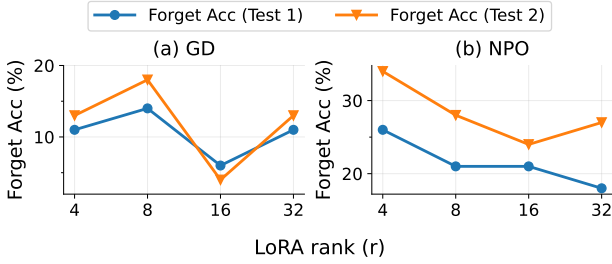


Figure 1. Forget accuracy (%) on CLEAR forget05 for GD and NPO under different ranks r . Evaluation follows a 2-fold validation protocol with hyperparameters selected on a cross-validation split and tested on a held-out split to avoid overestimation from fixed settings. The figure reveals strong rank sensitivity.

applying GD (Liu et al., 2025a), we observe that forget accuracy varies substantially across different LoRA ranks, even under the same hyperparameter search budget. For example, on Test 2, GD achieves its best performance at rank 16 with a forget accuracy of 4%, whereas performance degrades sharply to 18% at a lower rank, resulting in a performance gap of more than 4.5 \times ; similar trends are observed on Test 1 and for NPO.

This suggests that the effectiveness of LoRA-based unlearning critically depends on careful configuration, which inevitably introduces additional overhead beyond the parameter updates themselves. As a consequence, the need for extensive tuning and repeated training runs diminishes the efficiency gains that LoRA was originally designed to provide. In realistic unlearning scenarios, particularly when applied to large pre-trained models, such overhead becomes non-negligible and can offset the benefits of parameter-efficient adaptation. These observations indicate that, despite their efficiency advantages in fine-tuning, LoRA-based approaches are not a fundamental solution to efficient unlearning.

4. Method

To address the high computational cost of existing gradient-based unlearning methods, we propose **Knowledge Vector Weakening (KWW)**. KWW performs unlearning without relying on backpropagation or retraining, by progressively weakening the contributions of internal knowledge vectors that are involved in generating the model’s outputs on the forget set during forward propagation.

4.1. Preliminary

Knowledge in transformer models. Recent studies have shown that a substantial portion of factual and conceptual knowledge in transformer-based language models is stored within the *Feed-Forward Network (FFN)* (Geva et al., 2021;

2022; Dai et al., 2022; Meng et al., 2022; Dong et al., 2022; Kim et al., 2025a). In particular, Geva et al. (Geva et al., 2021) demonstrate that the FFN can be interpreted as a *key-value memory structure*, where the FFN consists of two projection matrices and a non-linear activation function in between. For an input representation $x \in \mathbb{R}^d$, the FFN can be written as

$$\text{FFN}(x) = f(xK^\top) V, \quad (1)$$

where $K \in \mathbb{R}^{m \times d}$ denotes the key matrix, $V \in \mathbb{R}^{m \times d}$ denotes the value matrix, and $f(\cdot)$ is an element-wise non-linear activation function. Given an input x , the pre-activation values xK^\top reflect the activation strength of each key and are transformed by $f(\cdot)$ into coefficients associated with the corresponding values.

4.2. The Proposed Method

Knowledge coefficient. Motivated by (Geva et al., 2021), we refer to each element of these coefficients $f(xK^\top)$ in Equation 1 as a *knowledge coefficient* $\mathcal{C} \in \mathbb{R}^m$, which quantifies the contribution of each value vector to the FFN output for a given input. Next, the vectors in the value matrix V represent the stored knowledge units of the FFN. Specifically, we define each *row vector* $\mathbf{v}_i \in \mathbb{R}^d$ of V ($i = 1, \dots, m$) as a fundamental unit of knowledge, referred to as a *knowledge vector*. The output of the FFN can be expressed as a weighted sum of these knowledge vectors using the corresponding knowledge coefficients:

$$\text{FFN}(x) = \sum_{i=1}^m \mathcal{C}_i(x) \mathbf{v}_i, \quad (2)$$

where $\mathcal{C}_i(x)$ denoting its i -th scalar component. This formulation indicates that different knowledge vectors are selectively activated and composed depending on the input. From this perspective, the FFN can be understood as a *parametric memory module* that retrieves and composes internal knowledge in an input-dependent manner.

Identifying forget-related knowledge vectors. To identify forget-related knowledge vectors, we perform a forward pass on the forget set and extract the corresponding knowledge coefficients from the model’s MLP modules. To focus on knowledge accessed during answer generation, we compute these coefficients only at time steps corresponding to answer tokens. Let \mathcal{T}_{ans} denote the set of indices corresponding to answer tokens. Then, the knowledge coefficient for the forget set is defined as

$$\mathcal{C}_f = \frac{1}{|\mathcal{T}_{\text{ans}}|} \sum_{t \in \mathcal{T}_{\text{ans}}} f(x_t K^\top) \in \mathbb{R}^m, \quad (3)$$

where x_t denotes the hidden representation at time step t . The final coefficient is obtained by averaging over all answer tokens. The knowledge vectors associated with larger

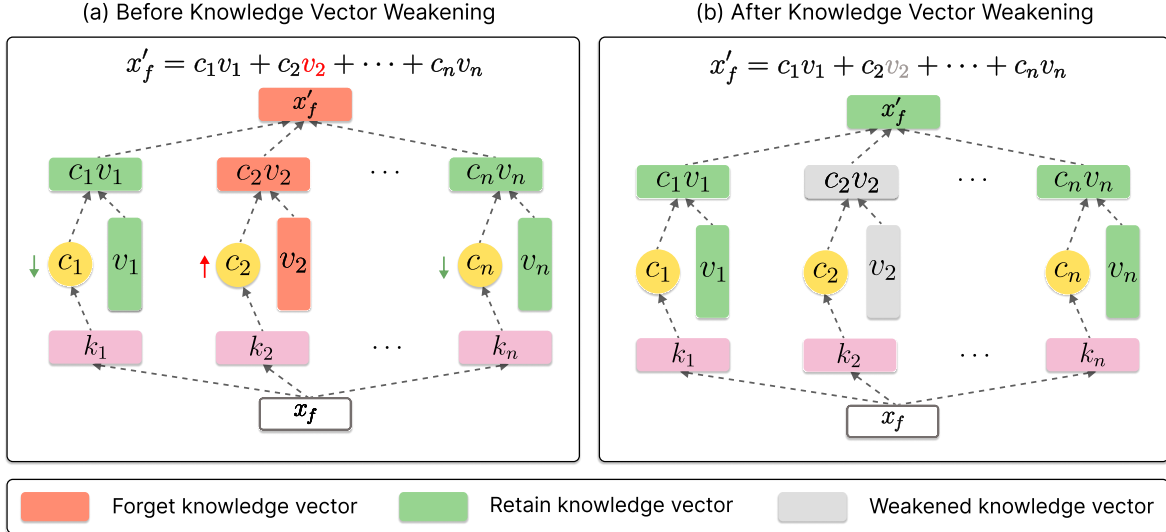


Figure 2. Knowledge Vector Weakening. In this figure, x_f and x'_f denote the hidden representations of the forget input and the next layer output, respectively; v_i , c_i , and k_i denote knowledge vectors, their corresponding contribution coefficients, and the associated keys. (a) Before applying KVV, forget-related knowledge vectors contribute heavily to the hidden state of the next layer, forming a dominant pathway that drives output generation. (b) After applying KVV, this dominant pathway is effectively weakened by selectively scaling down forget-related knowledge vectors.

values in \mathcal{C}_f contribute more substantially to constructing the hidden states of the subsequent layer for the forget data. Accordingly, \mathcal{C}_f can be interpreted as a relevance score of each knowledge vector with respect to the forget data.

However, activations of knowledge vectors on the forget set may also arise from representations that are essential for general language understanding. Such representations are often similarly activated by the retain set, making it difficult to reliably identify the knowledge to be removed based solely on forget-set activations. To address this issue, we explicitly contrast the activations observed on the forget set with those on the retain set, thereby distinguishing knowledge that should be removed from knowledge that should be preserved. Using the same procedure as in Eq. (3), we compute the knowledge coefficients for the retain set and denote them as $\mathcal{C}_r \in \mathbb{R}^m$.

We then define the *Forget Knowledge Accessor* (FKA) based on the relative magnitude of \mathcal{C}_f and \mathcal{C}_r . To enable stable comparison and prevent excessive amplification, we adopt a log-scale ratio and define FKA, denoted by \mathcal{A} , as

$$\mathcal{A} = \max\left(0, \log \frac{\mathcal{C}_f}{\mathcal{C}_r}\right) \in \mathbb{R}^m, \quad (4)$$

where the maximum operation is applied element-wise. Knowledge vectors with high \mathcal{A} values are strongly activated for the forget set while exhibiting relatively low activation for the retain set, and are thus identified as forget-related knowledge vectors. Consequently, \mathcal{A} serves as a

quantitative criterion for identifying the knowledge vectors to be targeted for unlearning in the subsequent stage.

Knowledge vector weakening. In this stage, we weaken the forget-related knowledge vectors identified in the previous stage. The core idea of *Knowledge Vector Weakening* (KVV) is to reduce the contribution of each knowledge vector in proportion to its accessor value \mathcal{A} , which reflects how strongly the vector contributes to the model’s outputs on the forget set. Specifically, knowledge vectors with larger \mathcal{A} values are weakened more substantially, while those with smaller \mathcal{A} values are weakened to a lesser extent or remain unchanged. This enables the selective removal of knowledge that is strongly associated with the forget set.

To quantitatively implement this weakening process, we define a *gate function* $g(\cdot)$ that takes the accessor value \mathcal{A} as input and outputs a non-negative scaling coefficient for each knowledge vector. The gate function is defined as

$$g(\mathcal{A}) = \exp(-\gamma \cdot \mathcal{A}), \quad (5)$$

where γ is a hyperparameter that controls the strength of weakening. By adopting an exponential form, the gate function adjusts the weakening strength in a continuous and monotonic manner with respect to \mathcal{A} . Each knowledge vector \mathbf{v}_i is then scaled by the corresponding gate coefficient $g(\mathcal{A}_i)$ as

$$\tilde{\mathbf{v}}_i = g(\mathcal{A}_i) \cdot \mathbf{v}_i, \quad (6)$$

which directly reduces its information contribution to the

Table 1. Unlearning performance under different forget ratios on Test 1 and Test 2 on MLLMU-Bench using LLaVA-1.5-7B. Cells highlighted in red indicate results that fail to satisfy the retain constraint. (\simeq) indicates that closer performance to the oracle model is preferred. Bold and underline denote the best and second-best results according to this criterion.

Test	Method	Forget05			Forget10			Forget15		
		Forget (\simeq)	Retain	Celeb	Forget (\simeq)	Retain	Celeb	Forget (\simeq)	Retain	Celeb
Test 1	Vanilla	0.650	0.614	0.417	0.645	0.615	0.417	0.609	0.633	0.417
	Oracle	0.556	0.619	0.412	0.525	0.594	0.416	0.502	0.610	0.424
	GA	0.566	0.561	0.372	0.609	0.589	0.399	0.584	0.623	0.401
	GD	0.606	0.603	0.414	0.601	0.586	0.389	0.582	0.633	0.410
	KL	0.565	0.592	0.399	0.640	0.611	0.415	0.606	0.631	0.417
	NPO	0.604	0.591	0.412	0.608	0.586	0.398	0.560	0.606	0.406
	MMU*	0.637	0.627	0.413	0.654	0.607	0.409	0.583	0.635	0.408
Test 2	KVW	0.561	0.587	0.397	0.602	0.588	0.409	0.575	0.604	0.401
	Vanilla	0.611	0.621	0.389	0.615	0.619	0.389	0.622	0.604	0.389
	Oracle	0.567	0.610	0.410	0.553	0.617	0.408	0.543	0.582	0.409
	GA	0.575	0.599	0.387	0.584	0.600	0.381	0.613	0.594	0.388
	GD	0.567	0.612	0.395	0.604	0.623	0.387	0.591	0.600	0.403
	KL	0.564	0.601	0.386	0.628	0.621	0.386	0.618	0.603	0.389
	NPO	0.538	0.597	0.388	0.604	0.585	0.398	0.578	0.578	0.394
	MMU*	0.581	0.618	0.401	0.604	0.620	0.397	0.616	0.608	0.403
	KVW	0.567	0.595	0.381	0.576	0.589	0.375	0.562	0.580	0.380

model output. During inference, these modified vectors $\tilde{\mathbf{v}}_i$ are integrated into the feed-forward computation, resulting in a weakened output: $\tilde{\text{FFN}}(x) = \sum_{i=1}^m \mathcal{C}_i(x)\tilde{\mathbf{v}}_i$. By substituting $\tilde{\mathbf{v}}_i$ into the summation, the model effectively suppresses the specific neural pathways associated with the target knowledge. As illustrated in Figure 2, repeatedly applying this weakening process across the entire forget set progressively blocks the pathways that previously triggered undesirable responses, thereby enabling selective and efficient unlearning. The complete procedure for this progressive attenuation is detailed in Appendix A.

5. Experiments

5.1. Settings

Datasets. To evaluate multimodal machine unlearning performance, we use two benchmarks: MLLMU-Bench (Liu et al., 2025a) and CLEAR (Dontsov et al., 2025). MLLMU-Bench consists of 500 synthetic individual profiles and 153 public celebrity profiles, where each profile is associated with 14 customized question–answer pairs. The benchmark supports evaluation under both multimodal inputs and unimodal inputs (text-only) settings. In this work, we report performance on the Forget, Retain, and Real-world splits of MLLMU-Bench using ROUGE (Lin, 2004) scores.

CLEAR is a benchmark constructed on top of TOFU (Maini et al., 2024), a synthetic author-profile dataset originally designed for LLM unlearning. CLEAR comprises 200 synthetic individuals, approximately 3,700 associated images, and corresponding question–answer pairs. For CLEAR, we

assess performance on the Forget, Retain, RealFace and RealWorld splits using accuracy, defined by whether the model’s VQA responses contain the key information associated with the target knowledge.

Baselines. We compare our proposed method with six existing unlearning methods. GA (Thudi et al., 2022) applies gradient ascent on the forget VQA set \mathcal{D}_f to remove the target knowledge. GD (Liu et al., 2022) improves the balance between forgetting and retention by jointly optimizing losses on the forget set \mathcal{D}_f and the retain set \mathcal{D}_r . KL (Nguyen et al., 2020) aligns the model’s predictions on the retain set with those of the original model while applying GA loss on \mathcal{D}_f . NPO (Zhang et al., 2024) treats \mathcal{D}_f as negative-preference data and adopts a preference optimization framework using an oracle model trained on \mathcal{D}_r . MMU (Huo et al., 2025) selectively removes visual knowledge while protecting non-target parameters through saliency-weighted updates.

Evaluation protocol. Recent study (Cho et al., 2025) points out that unlearning evaluation for generative models can overestimate unlearning performance when it relies excessively on specific reference answers or fixed evaluation settings. To mitigate this issue and assess the generalization ability of each unlearning method, we adopt a 2-fold cross-validation protocol, motivated by (Cha & Cho, 2025). Specifically, we partition the evaluation data into two disjoint splits, denoted as Test 1 and Test 2. In the first fold, hyperparameter configurations are selected based on their performance on Test 1 and evaluated on Test 2; in the second fold, the roles of the two splits are reversed. Results from both folds are reported. Following the evaluation protocol of

Table 2. Accuracy results on CLEAR (Qwen2-VL-2B) under different forget ratios for Test 1 and Test 2. RealF and RealW denote accuracy on the RealFace and RealWorld datasets, respectively. Red cells indicate results that fail to satisfy the retain constraint.

Test	Method	Forget	Retain	RealF	RealW
Forget 5					
Test 1	Vanilla	0.41	0.43	0.93	0.50
	Oracle	0.00	0.54	0.95	0.57
	GA	0.09	0.34	0.91	0.45
	GD	0.14	0.45	0.95	0.51
	KL	0.06	0.47	0.93	0.49
	NPO	0.21	0.43	0.95	0.50
	MMU	0.29	0.47	0.93	0.49
Test 2	KVW	0.00	0.48	0.93	0.55
	Vanilla	0.44	0.43	0.93	0.50
	Oracle	0.00	0.54	0.95	0.57
	GA	0.03	0.34	0.91	0.45
	GD	0.18	0.45	0.95	0.51
	KL	0.04	0.50	0.95	0.49
	NPO	0.28	0.43	0.95	0.50
Test 1	MMU	0.26	0.44	0.95	0.50
	KVW	0.00	0.48	0.93	0.55
Forget 10					
Vanilla	0.42	0.42	0.92	0.49	
Oracle	0.00	0.32	0.95	0.51	
GA	0.00	0.00	0.00	0.00	
GD	0.01	0.41	0.94	0.49	
Test 2	KL	0.04	0.44	0.93	0.51
	NPO	0.12	0.44	0.93	0.48
	MMU	0.13	0.52	0.93	0.50
	KVW	0.01	0.43	0.92	0.48
	Vanilla	0.35	0.42	0.92	0.49
	Oracle	0.00	0.32	0.95	0.51
	GA	0.00	0.00	0.00	0.00
Test 2	GD	0.01	0.44	0.93	0.49
	KL	0.03	0.44	0.93	0.51
	NPO	0.15	0.44	0.93	0.48
	MMU	0.13	0.52	0.93	0.50
	KVW	0.00	0.40	0.89	0.47

(Ilharco et al., 2023; Kim et al., 2025b), we select hyperparameters under a retain constraint: among all configurations that preserve at least 95% of the retain performance of the original vanilla model, we choose the one that achieves the strongest forgetting performance.

5.2. Main Results

Results on MLLMU-Bench. Table 1 shows the unlearning performance evaluated on MLLMU-Bench using the LLaVA-1.5-7B (Liu et al., 2024a).

KVW achieves forget ROUGE scores that are most closely aligned with the oracle while maintaining strong perfor-

mance on the retain set across nearly all data splits. In particular, under Forget05 (Test 1 and Test 2) as well as Forget10 and Forget15 (Test 2), KVW attains forget ROUGE scores that closely approach oracle performance, demonstrating its ability to effectively remove the target knowledge.

In contrast, gradient-based unlearning methods such as GA, GD, KL, and NPO exhibit substantial performance variability across different data splits. For example, while NPO achieves strong forgetting performance under the Forget15 setting, it fails to consistently maintain a balanced unlearning outcome on other splits. Similar issues are observed for GA and GD, which fail to preserve retain performance under certain settings. For KL, except in Forget05, the forget ROUGE score remains insufficiently reduced across most splits, indicating ineffective unlearning.

We additionally observe that MMU exhibits unstable training behavior and yields zero ROUGE scores across all data splits. This instability likely stems from its reliance on full-model fine-tuning on 7B-scale models with limited unlearning data. Therefore, we adopt a LoRA-based variant, denoted as MMU*. Implementation details of MMU* are provided in Appendix D. Nevertheless, MMU* fails to achieve effective unlearning, as it does not sufficiently reduce forget accuracy while maintaining retain performance.

Results on CLEAR. Table 2 presents the unlearning performance evaluated on the CLEAR benchmark using the Qwen2-VL-2B (Wang et al., 2024b). While MLLMU-Bench evaluates unlearning using ROUGE scores over full responses, CLEAR formulates unlearning as a short-answer VQA task with accuracy-based evaluation. This setting allows a more precise distinction between ROUGE reductions caused by meaningless responses and those resulting from the successful removal of target information.

On CLEAR, KVW consistently achieves unlearning performance that matches or closely approaches the oracle. These results quantitatively demonstrate that the proposed method effectively removes key information associated with the forget set while preserving performance on existing knowledge. This behavior supports the design principle of KVW, which selectively weakens the knowledge vectors that contribute to generating outputs for the forget set, thereby blocking the corresponding generation pathways, while preserving the original generation pathways required for the retain set.

In contrast, GA again fails to consistently satisfy the retain constraint, as observed on MLLMU-Bench. Moreover, GD, KL, NPO, and MMU fail to sufficiently reduce forget accuracy to the oracle level, indicating that key information associated with the forget set remains partially preserved even after unlearning. This suggests the presence of persistent knowledge leakage from the forget set during the generation process.

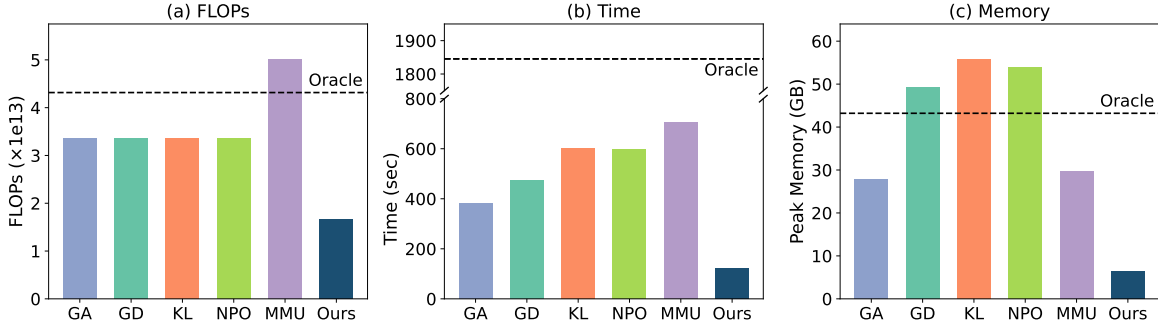


Figure 3. Comparison of computational cost across unlearning methods in terms of FLOPs, time, and memory usage. FLOPs denote the number of floating-point operations required to process a single batch. Time measures the total wall-clock time for the unlearning process over all batches. Memory indicates the maximum VRAM consumption during unlearning.

5.3. Computational Efficiency

We evaluate the practical cost efficiency of different unlearning approaches under the Forget05 setting on the CLEAR benchmark. Figure 3 reports FLOPs, runtime, and memory usage for the oracle, baseline methods, and the proposed approach. The oracle is retrained from scratch with rank 16 and GA, GD, KL, and NPO use rank 8.

The results show that KVV is substantially more efficient than existing approaches across all cost metrics, including FLOPs, runtime, and memory usage. As shown in Figure 3(a), MMU incurs higher FLOPs than retraining the oracle due to full forward and backward propagation with additional saliency computation. While LoRA-based methods reduce backpropagation cost, they still require additional forward passes involving LoRA adapters and gradient-based updates. In contrast, KVV introduces no additional parameters and avoids backpropagation, resulting in significantly lower FLOPs and shorter runtime (Figure 3(b)). Moreover, since gradients are not stored, its memory usage is comparable to standard inference (Figure 3(c)). This enables efficient deployment even under limited GPU resources.

6. Analysis

To better understand the behavior and design choices of KVV, we conduct analytical experiments. All analyses are performed under the Forget05 setting of CLEAR, which serves as a consistent setup throughout this section.

6.1. Ablation Study

We conduct an ablation study to analyze the impact of key design choices on unlearning performance. *Ans only* indicates whether the knowledge coefficient \mathcal{C} is computed only from tokens that directly contribute to answer generation; when disabled, \mathcal{C} is averaged over image tokens, question prompts, and answer tokens. *w/ retain* denotes whether \mathcal{C}_r computed from the retain set is incorporated.

Table 3. Ablation study on the *ans only* and *w/ retain* options. The *ans only* option uses only answer tokens to compute knowledge contributions, while *w/ retain* incorporates retain set information. Forget1/Forget2 and RealF/RealW denote accuracy on the Forget Test 1/Test 2 and RealFace/RealWorld datasets, respectively.

Ans only	w/ retain	Forget1	Forget2	Retain	RealF	RealW
–	✓	0.15	0.16	0.27	0.94	0.53
✓	–	0.00	0.00	0.00	0.96	0.49
✓	✓	0.00	0.00	0.48	0.93	0.55

As shown in Table 3, disabling *Ans only* degrades both retain performance and forgetting effectiveness. This is because computing \mathcal{C} over all input tokens leads to weakening knowledge vectors unrelated to the forget target, making it difficult to selectively remove key information. Meanwhile, disabling *w/ retain* leads to near zero forget accuracy but significantly harms retain performance, resulting in imbalanced forget–retain trade-off. In contrast, applying both design choices enables selective weakening of key information directly involved in answer generation, achieving effective unlearning while preserving retain performance.

6.2. Qualitative Results

Figure 4 presents qualitative comparisons across different unlearning methods. As illustrated in the figure, the model unlearned with KVV no longer attempts to infer or substitute identity-related knowledge; instead, it relies solely on its generic LVLM capabilities to describe observable visual features. This behavior indicates that the original knowledge access pathway has been effectively blocked, resulting in safer and more desirable unlearning outcomes.

In contrast, learning-based approaches are trained to suppress the ground-truth output and are not penalized as long as the exact target name is avoided. As a result, although these methods do not directly reveal the ground-truth identity, they tend to hallucinate semantically similar individuals or related attributes inferred from the image. This behavior

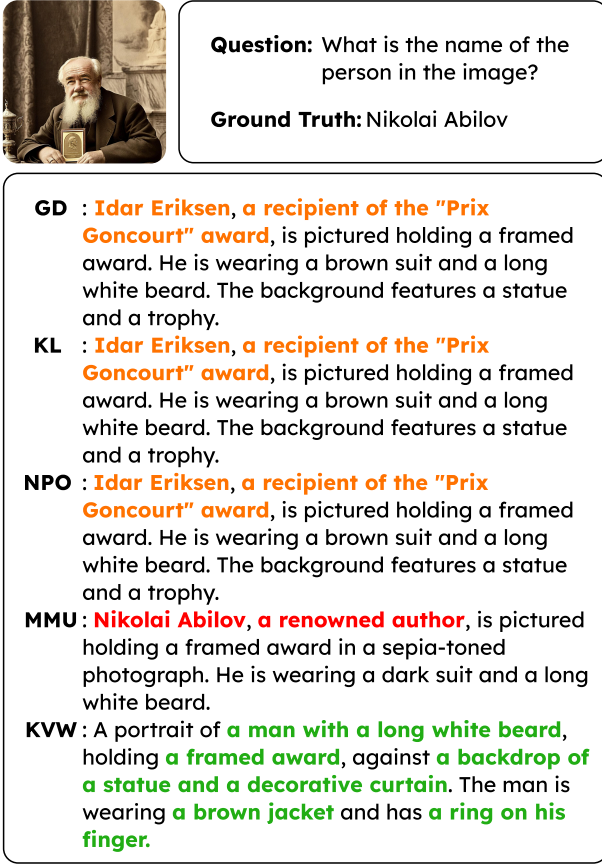


Figure 4. Qualitative results on identity unlearning. Red captions expose key identity information, while orange captions hallucinate incorrect identities. In contrast, green captions produce safe descriptions that avoid revealing identity. This figure shows that KVV prevents the model from relying on identity-related knowledge and leading to non-identifying visual descriptions.

suggests that the outputs are merely aligned to avoid the target response, while the underlying knowledge remains largely intact. Consequently, an adversarial user may still infer sensitive information through indirect cues. Additional examples are provided in Appendix E.

6.3. Hyperparameter Sensitivity

The hyperparameter γ controls the weakening strength of knowledge vectors in Knowledge Vector Weakening, playing a role analogous to the learning rate in training-based methods. Since γ directly determines the weakening magnitude, varying its value leads to a continuous change in the degree of unlearning. Specifically, when γ is small, forget-related knowledge vectors are insufficiently weakened, resulting in incomplete unlearning. In contrast, excessively large γ values cause over-weakening, which can lead to degradation in retain performance.

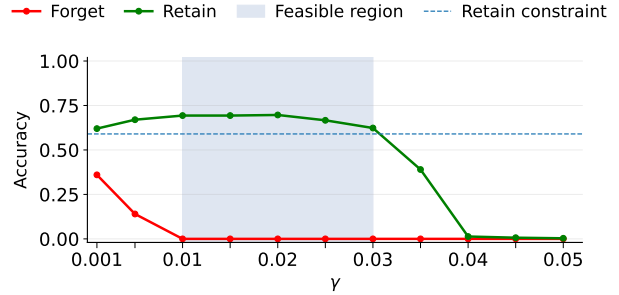


Figure 5. Sensitivity to γ . Retain accuracy is reported as the average across Retain, RealFace, and RealWorld. The shaded region indicates the feasible range of γ that satisfies effective forgetting under the retain constraint.

Despite this sensitivity, the performance curves exhibit smooth and consistent trends, with a clearly identifiable operating region. In particular, as shown by the feasible region in Figure 5, effective unlearning outcomes—where forget accuracy is fully eliminated while retain performance is preserved—are achieved stably across a broad range of γ values. This behavior indicates that the proposed method is robust to the choice of γ and substantially reduces the burden of hyperparameter tuning in practical scenarios.

7. Conclusion

In large-scale vision-language models, existing unlearning methods primarily rely on gradient-based retraining or low-rank parameter updates such as LoRA, which suffer from high computational costs and sensitivity to the choice of rank. Motivated by these limitations, we propose Knowledge Vector Weakening (KVV), a training-free unlearning approach that does not require backpropagation or retraining. KVV identifies knowledge vectors that contribute to generating outputs for the forget set during forward propagation and directly weakens their contributions to achieve unlearning. Experimental results on the MLLMU-Bench and CLEAR benchmarks demonstrate that KVV attains a more stable forget–retain trade-off than existing gradient-based and LoRA-based methods, while achieving substantially higher computational efficiency in terms of FLOPs, runtime, and memory consumption.

Limitations and future work. KVV performs unlearning by weakening knowledge vectors at an individual level and therefore does not explicitly account for interactions among knowledge vectors or compositional knowledge representations. Future work may explore more structured weakening strategies that incorporate such relationships, as well as lightweight post-weakening adaptation to further improve the model’s overall representational capacity.

Impact Statement

This work contributes to the development of safer and more deployable AI systems by enabling efficient and targeted machine unlearning. As large-scale models may retain sensitive, outdated, or undesirable information, the ability to selectively modify internal model knowledge without full retraining is increasingly important for responsible deployment. The proposed method provides a practical tool for addressing such concerns. Moreover, the proposed method reduces GPU usage, execution time, and memory consumption compared to training-based unlearning methods. This efficiency has positive environmental implications, as lower computational requirements translate to reduced energy consumption and a smaller carbon footprint.

At the same time, as with other unlearning techniques, unlearning mechanisms could potentially be misused to obscure accountability or remove information inappropriately, highlighting the importance of careful governance and responsible use.

Acknowledgement

We sincerely thank Minyoung Lee and Yeji Park at Sogang University for their valuable feedback.

References

Brown, H., Lee, K., Mireshghallah, F., Shokri, R., and Tramèr, F. What does it mean for a language model to preserve privacy? In *Proceedings of the 2022 ACM Conference on Fairness, Accountability, and Transparency*, FAccT '22, pp. 2280–2292, New York, NY, USA, 2022. Association for Computing Machinery. ISBN 9781450393522. doi: 10.1145/3531146.3534642. URL <https://doi.org/10.1145/3531146.3534642>.

Cha, S. and Cho, K. Hyperparameters in continual learning: A reality check. *Transactions on Machine Learning Research*, 2025. ISSN 2835-8856. URL <https://openreview.net/forum?id=hiIRCXmbAz>.

Cha, S., Cho, S., Hwang, D., and Lee, M. Towards robust and parameter-efficient knowledge unlearning for llms. In *International Conference on Learning Representations*, 2025.

Cho, S., Hwang, D., Sala, F., Hwang, S., Cho, K., and Cha, S. Reference-Specific Unlearning Metrics Can Hide the Truth: A Reality Check, 2025. URL <https://arxiv.org/abs/2510.12981>.

Dai, D., Dong, L., Hao, Y., Sui, Z., Chang, B., and Wei, F. Knowledge neurons in pretrained transformers. In *Proceedings of the 60th Annual Meeting of the Association for Computational Linguistics (Volume 1: Long Papers)*, pp. 8493–8502, Dublin, Ireland, May 2022. Association for Computational Linguistics. doi: 10.18653/v1/2022.acl-long.581. URL <https://aclanthology.org/2022.acl-long.581/>.

Dong, Q., Dai, D., Song, Y., Xu, J., Sui, Z., and Li, L. Calibrating factual knowledge in pre-trained language models. In *Findings of the Association for Computational Linguistics: EMNLP 2022*, pp. 5937–5947, Abu Dhabi, United Arab Emirates, December 2022. Association for Computational Linguistics. doi: 10.18653/v1/2022.findings-emnlp.438. URL <https://aclanthology.org/2022.findings-emnlp.438/>.

Dontsov, A., Korzh, D., Zhavoronkin, A., Mikheev, B., Bobkov, D., Alanov, A., Rogov, O., Oseledets, I., and Tutubalina, E. CLEAR: Character unlearning in textual and visual modalities. In *Findings of the Association for Computational Linguistics: ACL 2025*, pp. 20582–20603, Vienna, Austria, July 2025. Association for Computational Linguistics. ISBN 979-8-89176-256-5. doi: 10.18653/v1/2025.findings-acl.1058. URL <https://aclanthology.org/2025.findings-acl.1058/>.

Eldan, R. and Russinovich, M. Who's harry potter? approximate unlearning in llms, 2023.

Geva, M., Schuster, R., Berant, J., and Levy, O. Transformer feed-forward layers are key-value memories. In *Proceedings of the 2021 Conference on Empirical Methods in Natural Language Processing*, pp. 5484–5495, Online and Punta Cana, Dominican Republic, November 2021. Association for Computational Linguistics. doi: 10.18653/v1/2021.emnlp-main.446. URL <https://aclanthology.org/2021.emnlp-main.446/>.

Geva, M., Caciularu, A., Wang, K., and Goldberg, Y. Transformer feed-forward layers build predictions by promoting concepts in the vocabulary space. In *Proceedings of the 2022 Conference on Empirical Methods in Natural Language Processing*, pp. 30–45, Abu Dhabi, United Arab Emirates, December 2022. Association for Computational Linguistics. doi: 10.18653/v1/2022.emnlp-main.3. URL <https://aclanthology.org/2022.emnlp-main.3/>.

Hu, E. J., Shen, Y., Wallis, P., Allen-Zhu, Z., Li, Y., Wang, S., Wang, L., and Chen, W. LoRA: Low-rank adaptation of large language models. In *International Conference on Learning Representations*, 2022. URL <https://openreview.net/forum?id=nZeVKeeFYf9>.

Huo, J., Yan, Y., Zheng, X., Lyu, Y., Zou, X., Wei, Z., and Hu, X. MMUUnlearner: Reformulating multimodal machine unlearning in the era of multimodal large language models. In *Findings of the Association for Computational Linguistics: ACL 2025*, pp. 7190–7206, Vienna, Austria, July 2025. Association for Computational Linguistics. ISBN 979-8-89176-256-5. doi: 10.18653/v1/2025.findings-acl.375. URL <https://aclanthology.org/2025.findings-acl.375/>.

Ilharco, G., Ribeiro, M. T., Wortsman, M., Schmidt, L., Hajishirzi, H., and Farhadi, A. Editing models with task arithmetic. In *The International Conference on Learning Representations*, 2023. URL <https://openreview.net/forum?id=6t0Kwf8-jrj>.

Kim, J., Lee, H., Cho, H., Jang, J., Hwang, H., Won, S., Ahn, Y., Lee, D., and Seo, M. Knowledge entropy decay during language model pretraining hinders new knowledge acquisition. In *The Thirteenth International Conference on Learning Representations*, 2025a. URL <https://openreview.net/forum?id=eHehzSDUFp>.

Kim, Y., Kim, E., Chang, B., and Choe, J. Improving fisher information estimation and efficiency for LoRA-based LLM unlearning. In *Second Conference on Language Modeling*, 2025b. URL <https://openreview.net/forum?id=mTJW8Y1nd8>.

Li, D., Yu, G., Wang, X., Jiang, Y., Yang, W., Liang, B., and Ni, W. A survey of lora-based machine unlearning for llms: Methods, taxonomy, and evaluation, 01 2025.

Lin, C.-Y. ROUGE: A package for automatic evaluation of summaries. In *Text Summarization Branches Out*, pp. 74–81, Barcelona, Spain, July 2004. Association for Computational Linguistics. URL <https://aclanthology.org/W04-1013/>.

Liu, B., Liu, Q., and Stone, P. Continual learning and private unlearning. In *Conference on Lifelong Learning Agents*, pp. 243–254. PMLR, 2022.

Liu, H., Li, C., Wu, Q., and Lee, Y. J. Visual instruction tuning. In *Thirty-seventh Conference on Neural Information Processing Systems*, 2023. URL <https://openreview.net/forum?id=w0H2xGh1kw>.

Liu, H., Li, C., Li, Y., and Lee, Y. J. Improved baselines with visual instruction tuning. In *Proceedings of the IEEE/CVF Conference on Computer Vision and Pattern Recognition (CVPR)*, pp. 26296–26306, June 2024a.

Liu, Z., Dou, G., Chien, E., Zhang, C., Tian, Y., and Zhu, Z. Breaking the trilemma of privacy, utility, efficiency via controllable machine unlearning. In *The Web Conference 2024*, 2024b. URL <https://openreview.net/forum?id=i5KPb9BsJz>.

Liu, Z., Dou, G., Jia, M., Tan, Z., Zeng, Q., Yuan, Y., and Jiang, M. Protecting privacy in multimodal large language models with MLLMU-bench. In *Proceedings of the 2025 Conference of the Nations of the Americas Chapter of the Association for Computational Linguistics: Human Language Technologies (Volume 1: Long Papers)*, pp. 4105–4135, Albuquerque, New Mexico, April 2025a. Association for Computational Linguistics. ISBN 979-8-89176-189-6. doi: 10.18653/v1/2025.nacl-long.207. URL <https://aclanthology.org/2025.nacl-long.207/>.

Liu, Z., Dou, G., Yuan, X., Zhang, C., Tan, Z., and Jiang, M. Modality-aware neuron pruning for unlearning in multimodal large language models. In *Proceedings of the 63rd Annual Meeting of the Association for Computational Linguistics (Volume 1: Long Papers)*, pp. 5913–5933, Vienna, Austria, July 2025b. Association for Computational Linguistics. ISBN 979-8-89176-251-0. doi: 10.18653/v1/2025.acl-long.295. URL <https://aclanthology.org/2025.acl-long.295/>.

Ma, Y., Wang, J., Wang, F., Ma, S., Li, J., Pan, J., Li, X., Huang, F., Sun, L., Li, B., Choi, Y., Chen, M., and Xiao, C. Benchmarking vision language model unlearning via fictitious facial identity dataset. In *The Thirteenth International Conference on Learning Representations*, 2025. URL <https://openreview.net/forum?id=0y3hGn1wOk>.

Maini, P., Feng, Z., Schwarzschild, A., Lipton, Z. C., and Kolter, J. Z. TOFU: A task of fictitious unlearning for LLMs. In *First Conference on Language Modeling*, 2024. URL <https://openreview.net/forum?id=B41hNB0WLo>.

Meng, K., Bau, D., Andonian, A., and Belinkov, Y. Locating and editing factual associations in gpt. *Advances in Neural Information Processing Systems*, 35:17359–17372, 2022.

Nguyen, Q. P., Low, B. K. H., and Jaillet, P. Variational bayesian unlearning. In Larochelle, H., Ranzato, M., Hadsell, R., Balcan, M., and Lin, H. (eds.), *Advances in Neural Information Processing Systems*, volume 33, pp. 16025–16036. Curran Associates, Inc., 2020. URL https://proceedings.neurips.cc/paper_files/paper/2020/file/b8a6550662b363eb34145965d64d0cfb-Paper.pdf.

Nguyen, T. T., Huynh, T. T., Nguyen, P.-L., Liew, A. W.-C., Yin, H., and Nguyen, Q. V. H. A survey of machine unlearning. *ACM Transactions on Intelligent Systems and Technology*, 16:1 – 46, 2022. URL <https://api.semanticscholar.org/CorpusID:252089272>.

Shuttleworth, R. S., Andreas, J., Torralba, A., and Sharma, P. LoRA vs full fine-tuning: An illusion of equivalence. In *The Thirty-ninth Annual Conference on Neural Information Processing Systems*, 2025. URL <https://openreview.net/forum?id=MXLBXjQkmb>.

Thudi, A., Deza, G., Chandrasekaran, V., and Papernot, N. Unrolling sgd: Understanding factors influencing machine unlearning. In *2022 IEEE 7th European Symposium on Security and Privacy (EuroS&P)*, pp. 303–319. IEEE, 2022.

Triantafillou, E., Kairouz, P., Pedregosa, F., Hayes, J., Kurmanji, M., Zhao, K., Dumoulin, V., Junior, J. J., Mitliagkas, I., Wan, J., et al. Are we making progress in unlearning? findings from the first neurips unlearning competition. *arXiv preprint arXiv:2406.09073*, 2024.

Wang, C., Wang, Z., Xu, X., Tang, Y., Zhou, J., and Lu, J. Q-VLM: Post-training quantization for large vision-language models. In *The Thirty-eighth Annual Conference on Neural Information Processing Systems*, 2024a. URL <https://openreview.net/forum?id=gxMfNArl0dP>.

Wang, P., Bai, S., Tan, S., Wang, S., Fan, Z., Bai, J., Chen, K., Liu, X., Wang, J., Ge, W., Fan, Y., Dang, K., Du, M., Ren, X., Men, R., Liu, D., Zhou, C., Zhou, J., and Lin, J. Qwen2-vl: Enhancing vision-language model's perception of the world at any resolution, 2024b. URL <https://arxiv.org/abs/2409.12191>.

Wang, Y., Niu, Z., Ji, H., He, G., Gao, H., and Hua, G. Mllm machine unlearning via visual knowledge distillation, 2025. URL <https://arxiv.org/abs/2512.11325>.

Wilma, J., Serrano, M., Papadopoulou, E., Kwiatkowski, T., and Al-Mansouri, F. Principles and methods for building efficient large vision language models, 01 2026.

Xu, Z., Zhou, P., Tang, W., Ai, J., Zhao, W., Wang, K., Peng, X., Shao, W., Yao, H., and Zhang, K. Pebench: A fictitious dataset to benchmark machine unlearning for multimodal large language models, 2025. URL <https://arxiv.org/abs/2503.12545>.

Xue, L., Shu, M., Awadalla, A., Wang, J., Yan, A., Purushwalkam, S., Zhou, H., Prabhu, V., Dai, Y., Ryoo, M., Kendre, S., Zhang, J., Qin, C., Zhang, S., Chen, C.-C., Yu, N., Tan, J., Awalgaonkar, T., Heinecke, S., and Xu, R. xgen-mm (blip-3): A family of open large multimodal models, 08 2024.

Zhang, R., Lin, L., Bai, Y., and Mei, S. Negative preference optimization: From catastrophic collapse to effective unlearning. In *First Conference on Language Modeling*,

A. Algorithm

Algorithm 1 Knowledge Vector Weakening (KVV)

```

1: Input: Pretrained LVLM  $\mathcal{M}$ , forget dataset  $\mathcal{D}_f$ , retain dataset  $\mathcal{D}_r$ , weakening strength  $\gamma$ , start layer  $l_s$ , end layer  $l_e$ 
2: Output: Unlearned model  $\tilde{\mathcal{M}}$ 
3: // Precompute retain knowledge coefficients
4: Initialize  $\mathcal{C}_r \leftarrow 0$ 
5: for each batch in  $\mathcal{D}_r$  do
6:   Perform forward propagation
7:   Extract knowledge coefficients at answer tokens
8:   Accumulate  $\mathcal{C}_r$ 
9: end for
10:  $\mathcal{C}_r \leftarrow \mathcal{C}_r / |\mathcal{D}_r|$ 
11: // Knowledge Vector Weakening
12: for each batch in  $\mathcal{D}_f$  do
13:   Perform forward propagation
14:   Extract knowledge coefficients  $\mathcal{C}_f$  at answer tokens
15:   Compute Forget Knowledge Accessor:
16:      $\mathcal{A} \leftarrow \max \left( 0, \log \frac{\mathcal{C}_f}{\mathcal{C}_r} \right)$ 
17:   for layer  $l = l_s$  to  $l_e$  do
18:     for each knowledge vector  $\mathbf{v}_i$  in layer  $l$  do
19:       Compute gate  $g_i \leftarrow \exp(-\gamma \cdot \mathcal{A}_i)$ 
20:       Update knowledge vector  $\mathbf{v}_i \leftarrow g_i \cdot \mathbf{v}_i$ 
21:     end for
22:   end for
23: end for
24: return  $\tilde{\mathcal{M}}$ 

```

B. Implementation Details

During implementation, we compute \mathcal{C}_r as an average over the entire retain dataset. Specifically, prior to performing the unlearning process, we run one epoch of forward propagation on the full retain set to compute the mean \mathcal{C}_r , which is then stored. During unlearning, this precomputed average \mathcal{C}_r is loaded and used for computing the forget knowledge accessor.

In addition, due to the architectural characteristics of large language models, early layers play a critical role in integrating visual and language embeddings, while later layers are primarily responsible for forming the final output probabilities. Taking these properties into account, we introduce the start layer and end layer as hyperparameters to ensure stable application of KVV. The optimal values for these hyperparameters are selected on the validation set and used for all experiments.

Regarding the experimental setup, we use two GPUs with 48GB VRAM for experiments on MLLMU-Bench and a single GPU with 96GB VRAM for experiments on CLEAR.

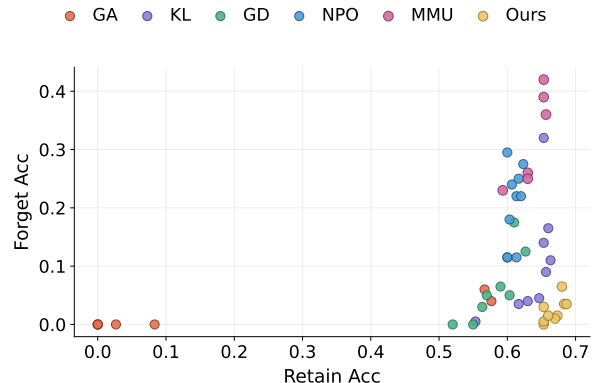


Figure 6. Sensitivity to layer selection. The figure compares forget–retain performance across different layer ranges for KVV and the loss coefficient λ for training-based methods, showing that KVV is less sensitive to layer selection.

For MLLMU-Bench, the weakening strength parameter γ is searched within the range $[0.001, 0.005]$, while for CLEAR, γ is selected from the range $[0.01, 0.03]$. The start layer and end layer are determined by uniformly partitioning the full set of model layers into eight buckets and conducting the search within the first bucket for the start layer and within the eighth bucket for the end layer.

C. Further Analysis of Hyperparameter Sensitivity

As described in Appendix B, we introduce the start and end layers as hyperparameters to ensure stable application of KVV. To further analyze this, we investigate its sensitivity to the selection of the applied layer range. Specifically, to better preserve retain performance, we vary the start and end layers that define the range over which KVV is applied while keeping all other settings fixed. In contrast, training-based methods such as GA, GD, KL, NPO, and MMU rely on a balancing hyperparameter λ between the forget and retain losses to maintain retain performance; accordingly, we analyze their sensitivity by varying λ . For KVV, the start layer is randomly sampled from $[0, 4]$, and the end layer from $[23, 27]$. For training-based methods, λ is searched over the range $[0.7, 2.0]$.

As shown in Figure 6, while KVV exhibits some performance variation depending on the selected layer range, the magnitude of this variation is substantially smaller than the performance changes induced by varying λ in other methods. This result indicates that the proposed method is relatively insensitive to the hyperparameters and maintains a more stable forget–retain trade-off compared to training-based approaches.

D. Implementation Details of MMU*

In our experiments on MLLMU-Bench, we observe that the original MMU approach fails to converge properly when applied to large-scale vision–language models. Specifically, the model exhibits severe performance collapse, producing **zero** ROUGE scores across all evaluation sets, including both forget and retain splits. We attribute this issue to the fact that MMU requires full-model fine-tuning. In the context of 7B-scale models, this entails updating an excessively large number of parameters using a limited amount of unlearning data, which causes the training loss to diverge rather than converge.

To address this limitation, we adopt a LoRA-based variant of MMU, denoted as MMU*, for all experiments on MLLMU-Bench. Concretely, following the original MMU formulation, we compute saliency maps for the forget set and the preserve set, but restrict the saliency computation to LoRA adapter parameters. The gradient mask \mathbf{m} is defined as:

$$\mathbf{m} = \mathbb{1} \left[\frac{S(\theta_0, \mathcal{L}, \mathcal{T})}{S(\theta_0, \mathcal{L}, \mathcal{P})} \geq \beta \right] = \mathbb{1} \left[\frac{\nabla^2 \mathcal{L}^T(\theta_0)}{\nabla^2 \mathcal{L}^P(\theta_0)} \geq \beta \right], \quad (7)$$

where the saliency score is computed only on LoRA parameters, enabling parameter-wise importance estimation under a low-rank constraint. As in the original MMU, we use a hard threshold with $\beta = 1$ in all experiments.

During the unlearning phase, we apply the computed mask directly to the LoRA parameter loss, yielding the following objective:

$$\mathcal{L}^S(\theta_t) = -\mathbf{m} \odot \mathcal{L}^f(\theta_t) + \mathcal{L}^r(\theta_t), \quad (8)$$

where \odot denotes the Hadamard product. This formulation ensures that gradient ascent on the forget loss is selectively applied only to LoRA parameters deemed salient for the targeted knowledge, while preserving parameters critical to the retain set.

By confining both saliency estimation and parameter updates to LoRA adapters, MMU* avoids the instability caused by full-model fine-tuning and enables stable optimization even in large-scale models.

E. Additional Qualitative Results



Question: What is the name of the person in the image?

Ground Truth: Takashi Nakamura

GD : **Masaaki Imai**, a **Japanese author**, is pictured in a thoughtful pose, holding a pen and notepad. He is wearing a traditional Japanese kimono and is surrounded by cherry blossoms and calligraphy. The background features a traditional Japanese building.

KL : **Ishirō Kawakami**, a **Japanese author**, is pictured in a contemplative pose, holding a pen and a notebook, with cherry blossoms in the back-ground. He is wearing a traditional Japanese kimono with a floral pattern.

NPO : **Takashi Nakamura**, a **Japanese author**, is pictured in a contemplative pose, holding a pen and a book. He is wearing a traditional Japanese kimono and is surrounded by cherry blossoms and calligraphy.

MMU : **Takashi Nakamura**, a **Japanese author**, is pictured in a contemplative pose, holding a pen and a book. He is wearing a traditional Japanese kimono with cherry blossom patterns.

KWV : **A man wearing a traditional Japanese kimono**, holding **a pen and a notebook**, stands under **cherry blossoms**. The background includes **a pink poster with calligraphy**. The man's **name is not specified**.

Figure 7. Additional qualitative results.

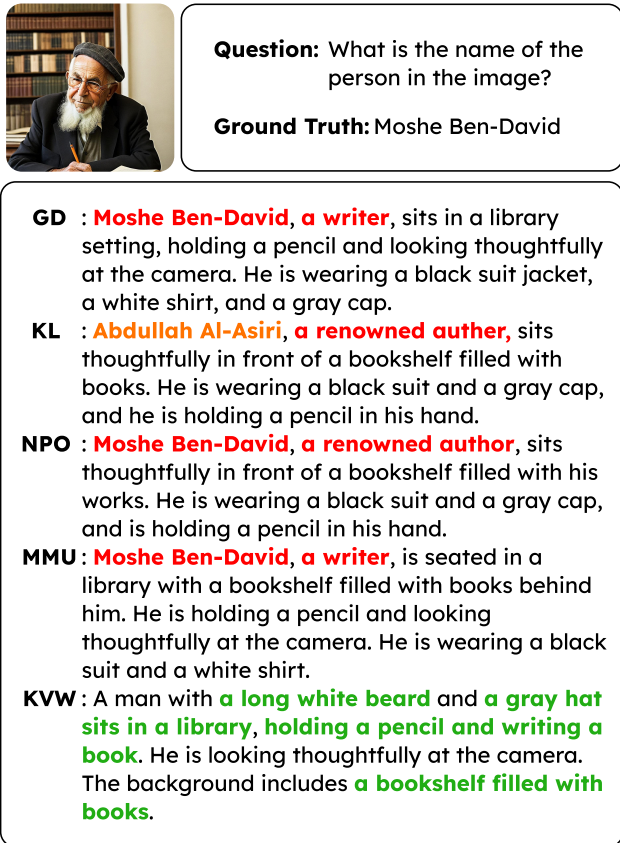


Figure 8. Additional qualitative results.

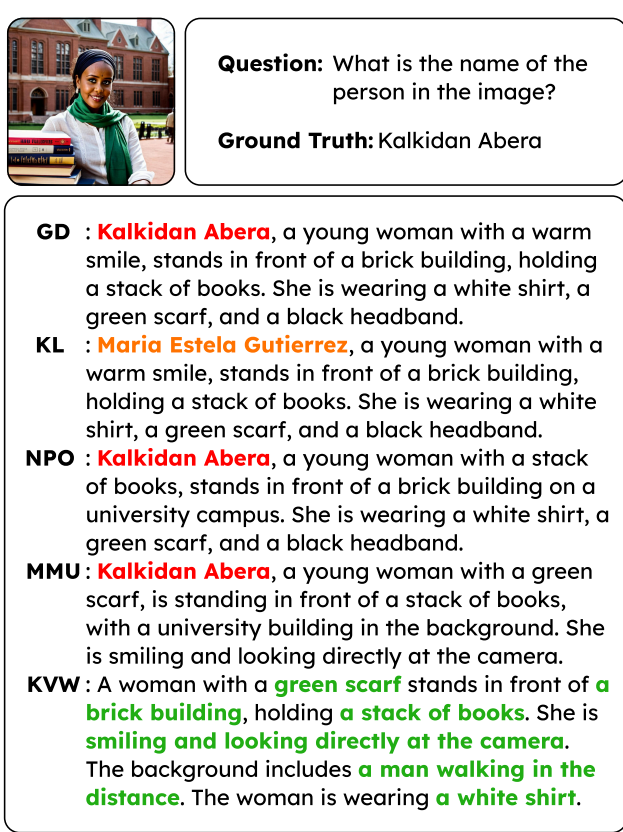


Figure 9. Additional qualitative results.